

# Co<sub>3</sub>O<sub>4</sub>/Activated Carbon Nanocomposites as Electrocatalysts for Oxygen Evolution Reaction

Andrei F. V. de Lima,<sup>a</sup> Annaíres de A. Lourenço,<sup>a</sup> Vinícius D. Silva,<sup>b</sup> André L. Menezes de Oliveira,<sup>c</sup> Arpad M. Rostas,<sup>d</sup> Lucian Barbu Tudoran,<sup>d</sup> Cristian Leostean,<sup>d</sup> Ovidiu Pana,<sup>d</sup> Rodolfo B. da Silva,<sup>b</sup> Daniel A. Macedo,<sup>b</sup> Fausthon F. da Silva,<sup>\*a</sup>

---

*a. Departamento de Química, Universidade Federal da Paraíba, 58051-900, João Pessoa-PB, Brazil.*

*b. Programa de Pós-Graduação em Ciência e Engenharia de Materiais – PPECM, Universidade Federal da Paraíba, 58051-900, João Pessoa-PB, Brazil.*

*c. Núcleo de Pesquisa e Extensão LACOM, Departamento de Química, Universidade Federal da Paraíba, 52051-85, João Pessoa-PB, Brazil*

*d. Department of Physics of Nanostructure Systems, National Institute for Research and Development of Isotopic and Molecular Technologies, 400293 Cluj-Napoca, Romania.*

## Electronic Supplementary Information

**Table S1.** Mass of the ZIF-67/C products, mass and yield of ZIF-67 obtained in the synthesis, and percentage (w/w) of ZIF-67 in the composites.

Samples	product	Activated carbon	ZIF-67	Yield of ZIF-67	%(w/w <sub>total</sub> ) of ZIF-67 in the composite
ZIF-67/C10	228 mg	117 mg	111 mg	40.4%	48.7%
ZIF-67/C30	480 mg	351 mg	129 mg	46.9%	26.9%
ZIF-67/C50	716 mg	581 mg	135 mg	49.1%	18.9%
ZIF-67*	135 mg	--	--	49.1%	--

\*Synthesis without the presence of activated carbon

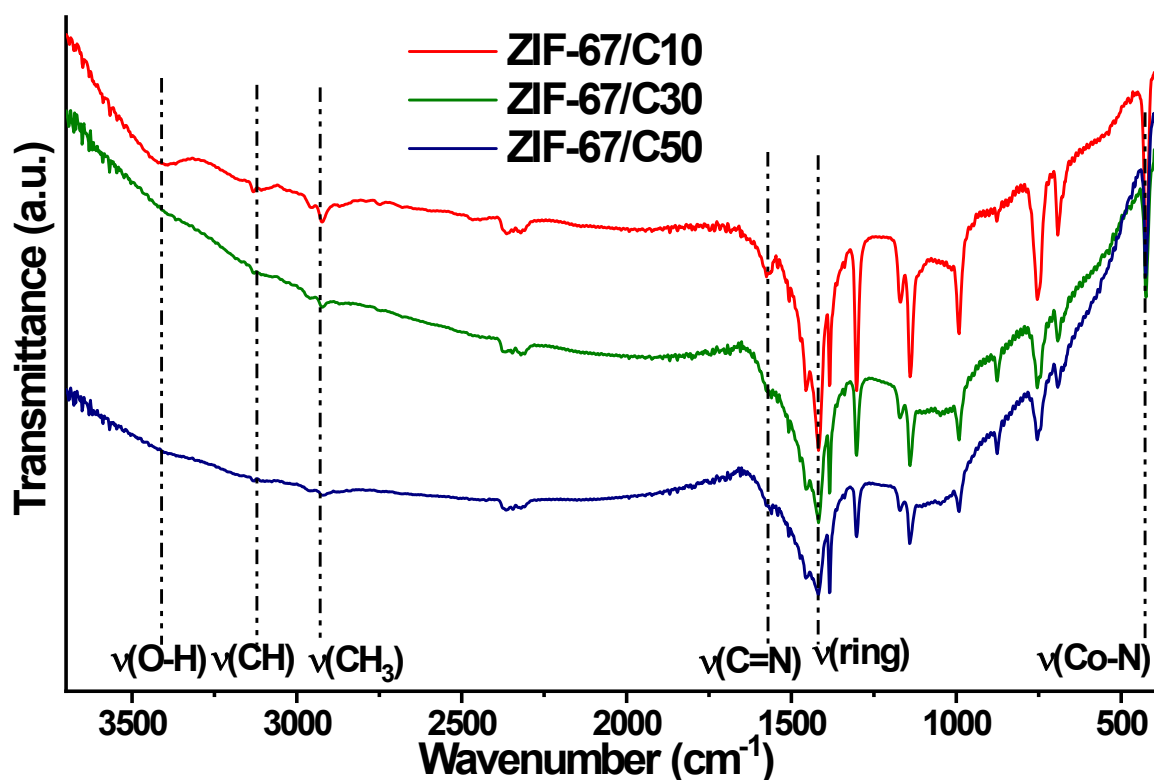


**Figure S1:** FT-IR spectra of the ZIF-67/C composites

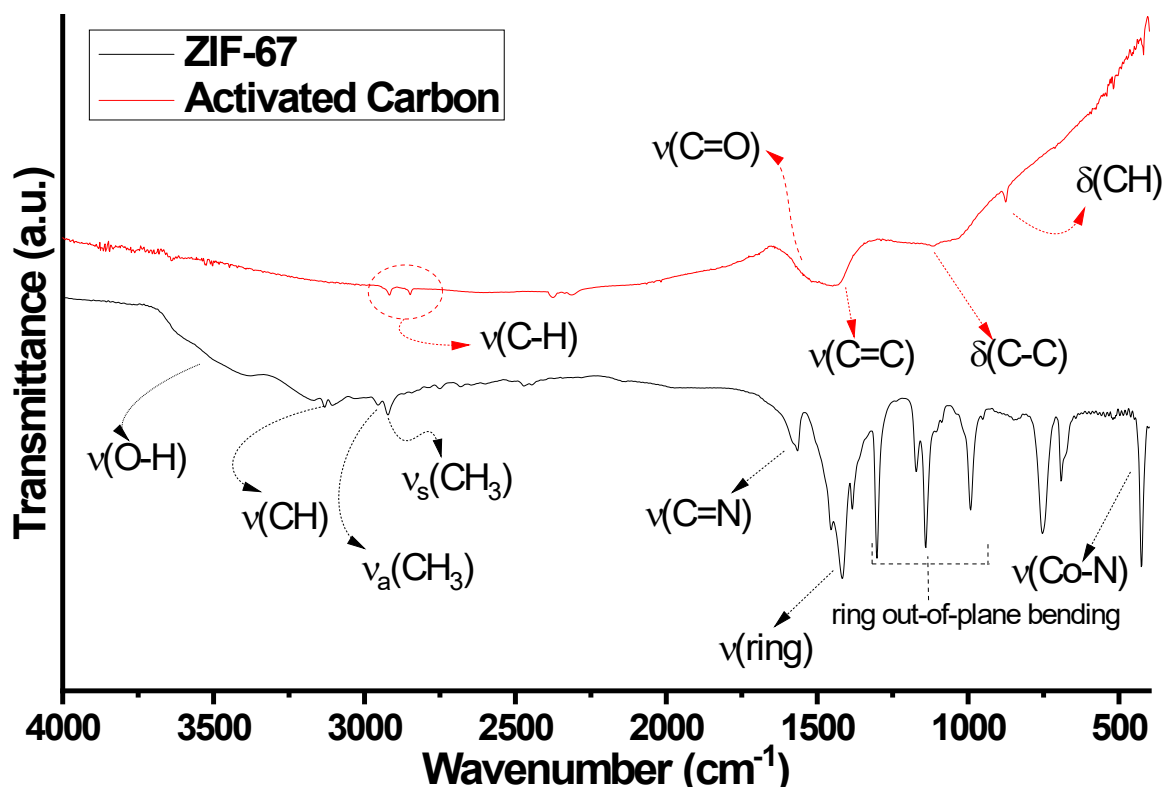


Figure S2: FT-IR spectra of activated carbon and ZIF-67.

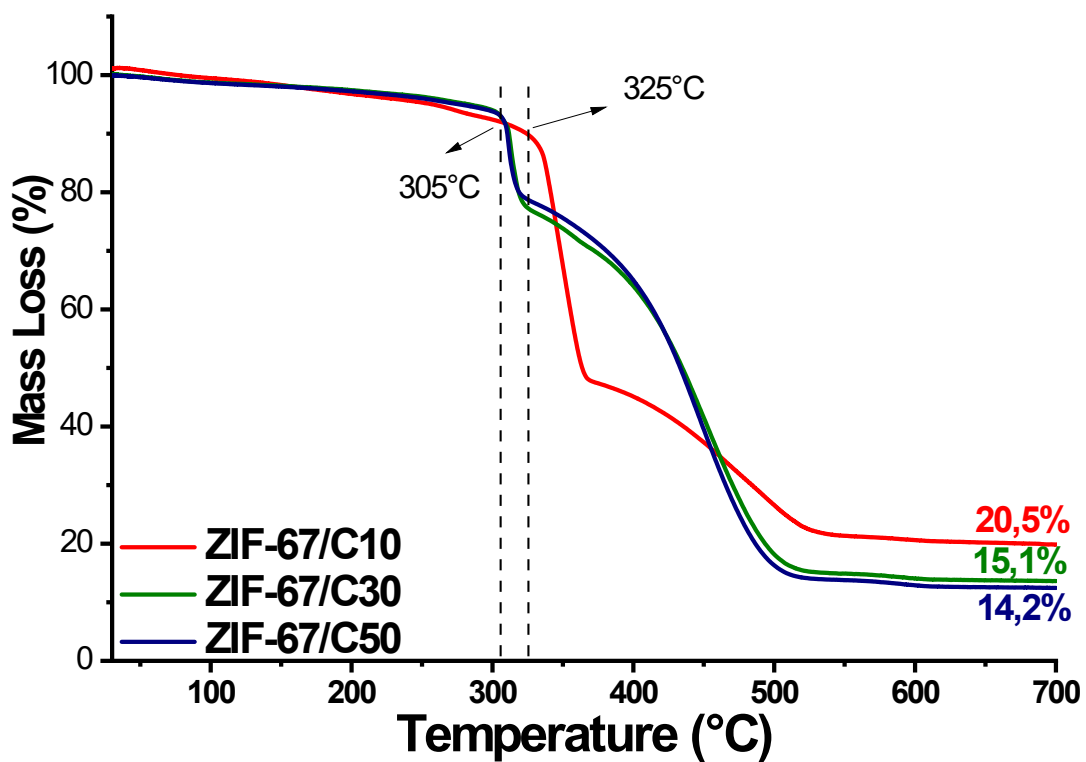
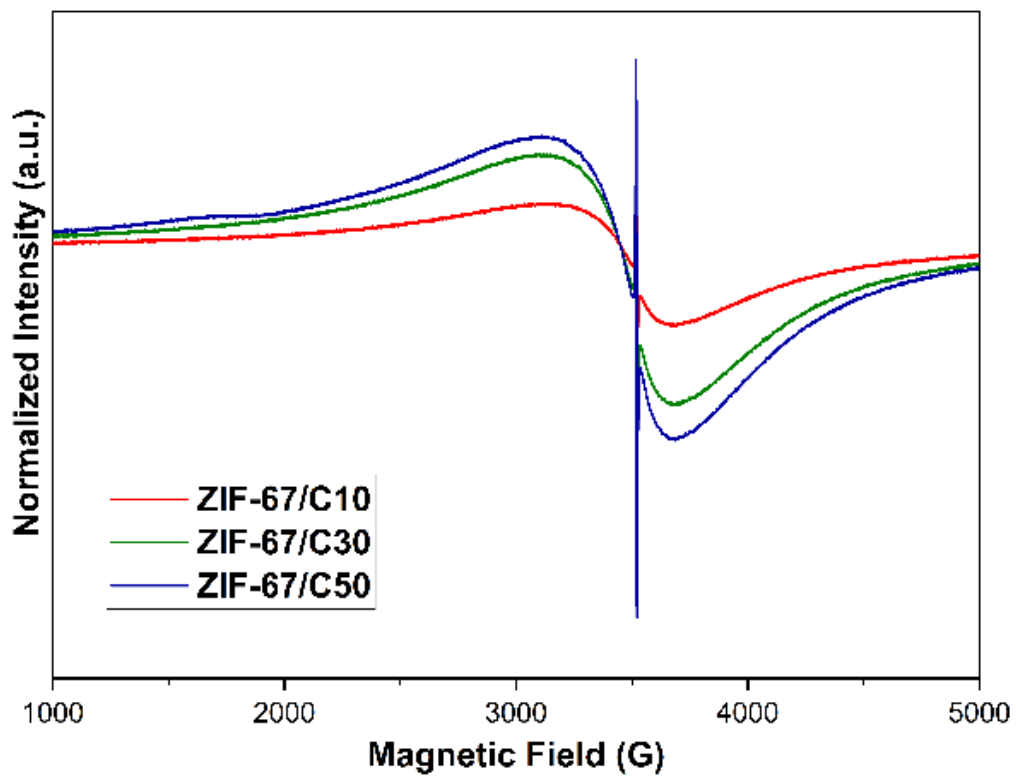
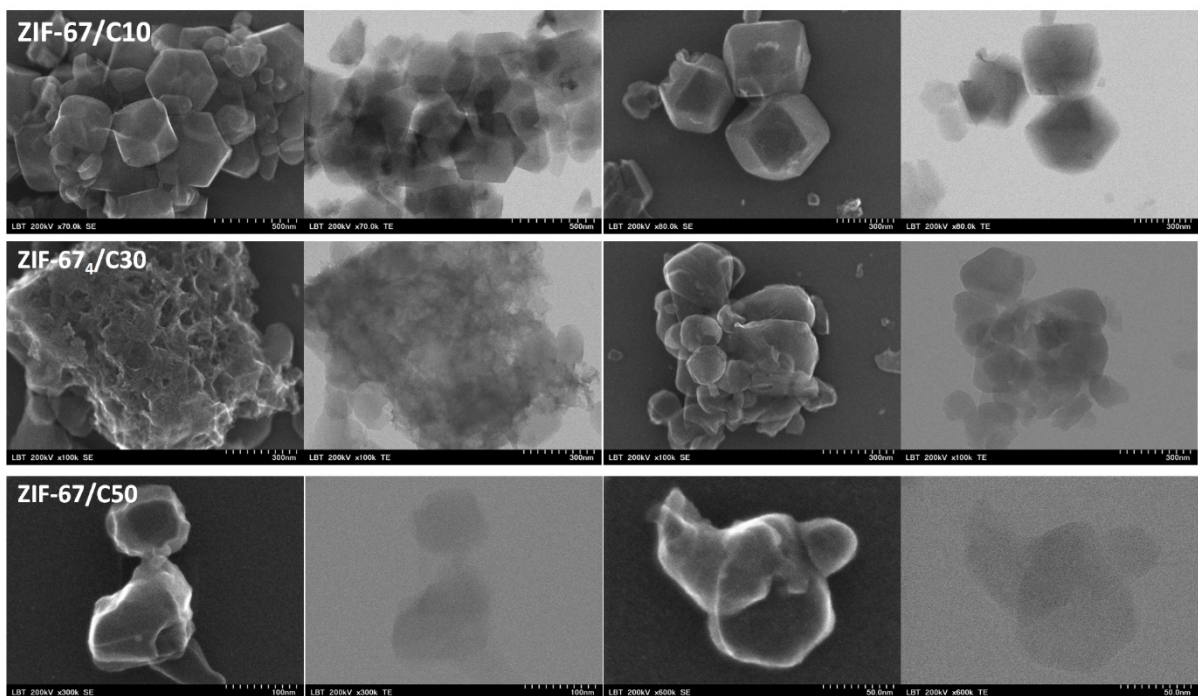


Figure S3: TGA curves of ZIF-67/C composites.



**Figure S4:** EPR spectra of ZIF-67/C composites.



**Figure S5:** S-TEM images of collected for ZIF-67/C nanocomposites.

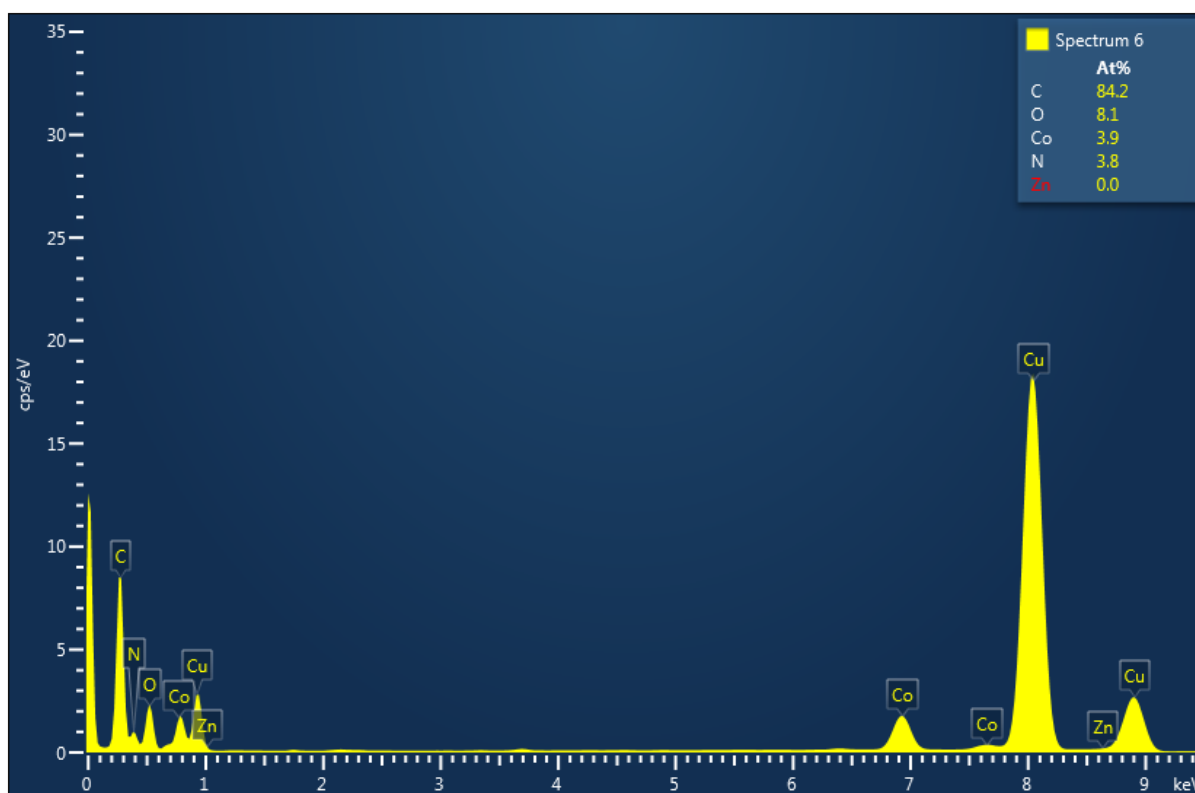


**Figure S6:** EDS spectra of the ZIF-67/C10 composite.  
\*Cu signals are related to the TEM grid sample holder.

**Table S2.** Cell parameters and crystallite size of  $\text{Co}_3\text{O}_4/\text{C}$  nanocomposites obtained from the Rietveld refinement.

Samples	$a = b = c$ (Å)	Crystallite size (nm)	Volume (Å <sup>3</sup> )
$\text{Co}_3\text{O}_4$ (ICSD – 150805)	8.0800	--	527.51
$\text{Co}_3\text{O}_4/\text{C10}$	8.0807±0.003	13.94	527.65
$\text{Co}_3\text{O}_4/\text{C30}$	8.0773±0.003	13.20	526.99
$\text{Co}_3\text{O}_4/\text{C50}$	8.0770±0.002	15.27	526.93

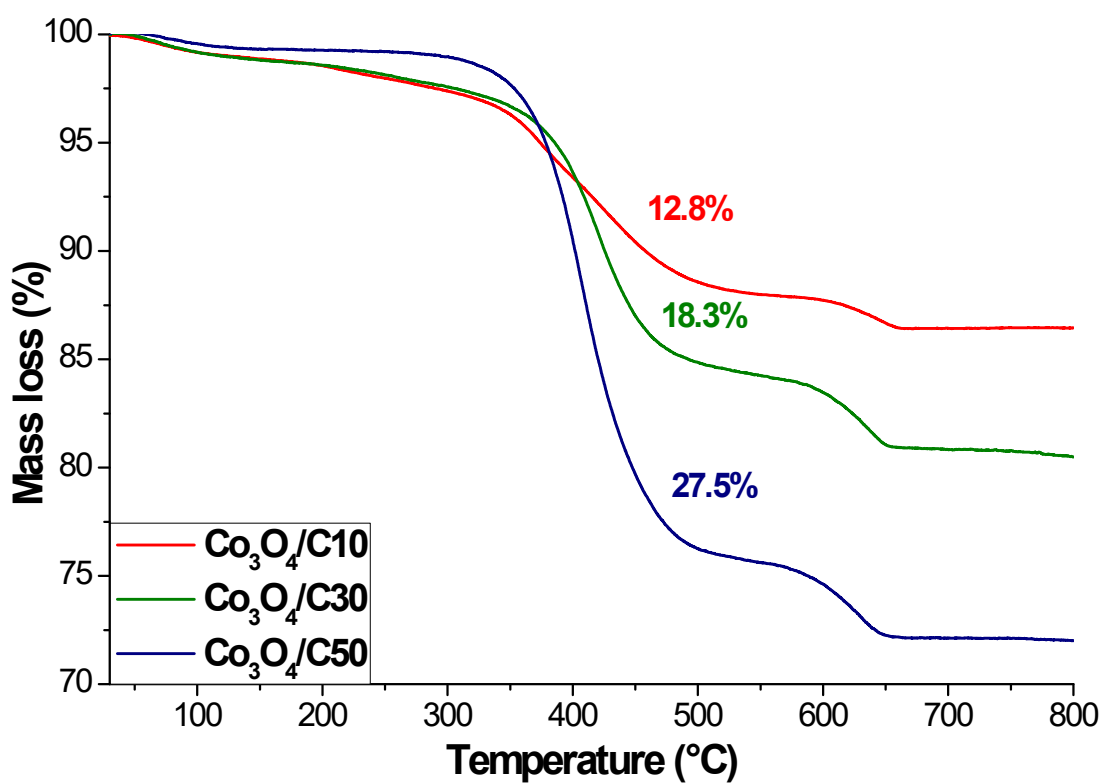


Figure S7: TGA curves of  $\text{Co}_3\text{O}_4/\text{C}$  composites.

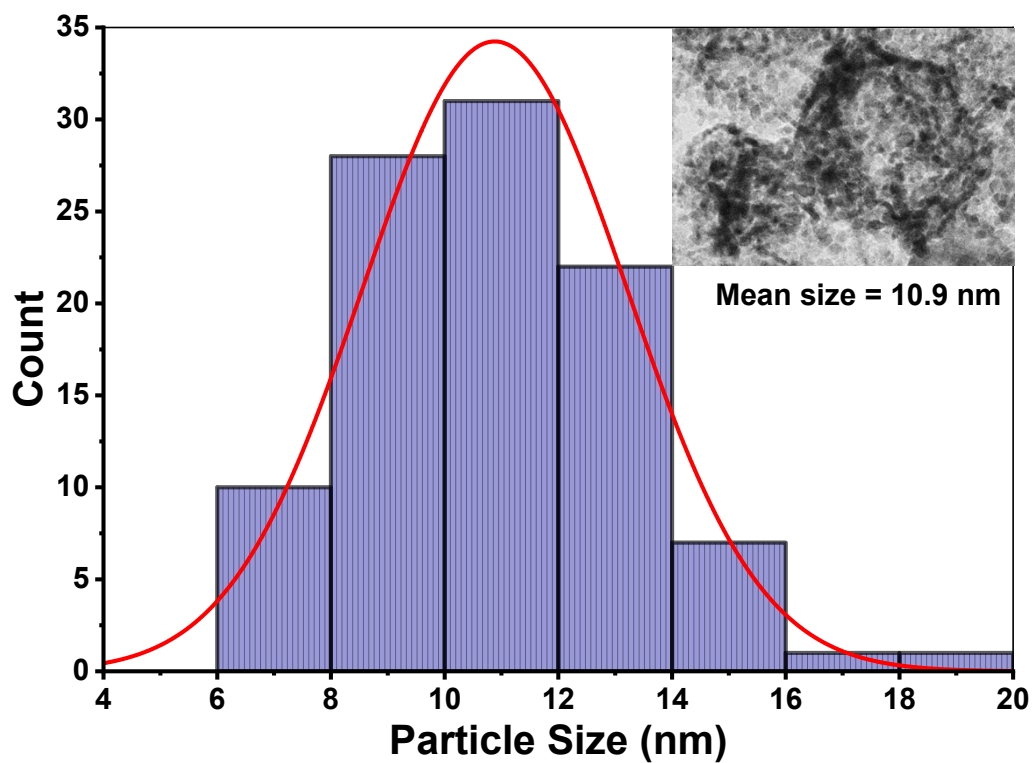
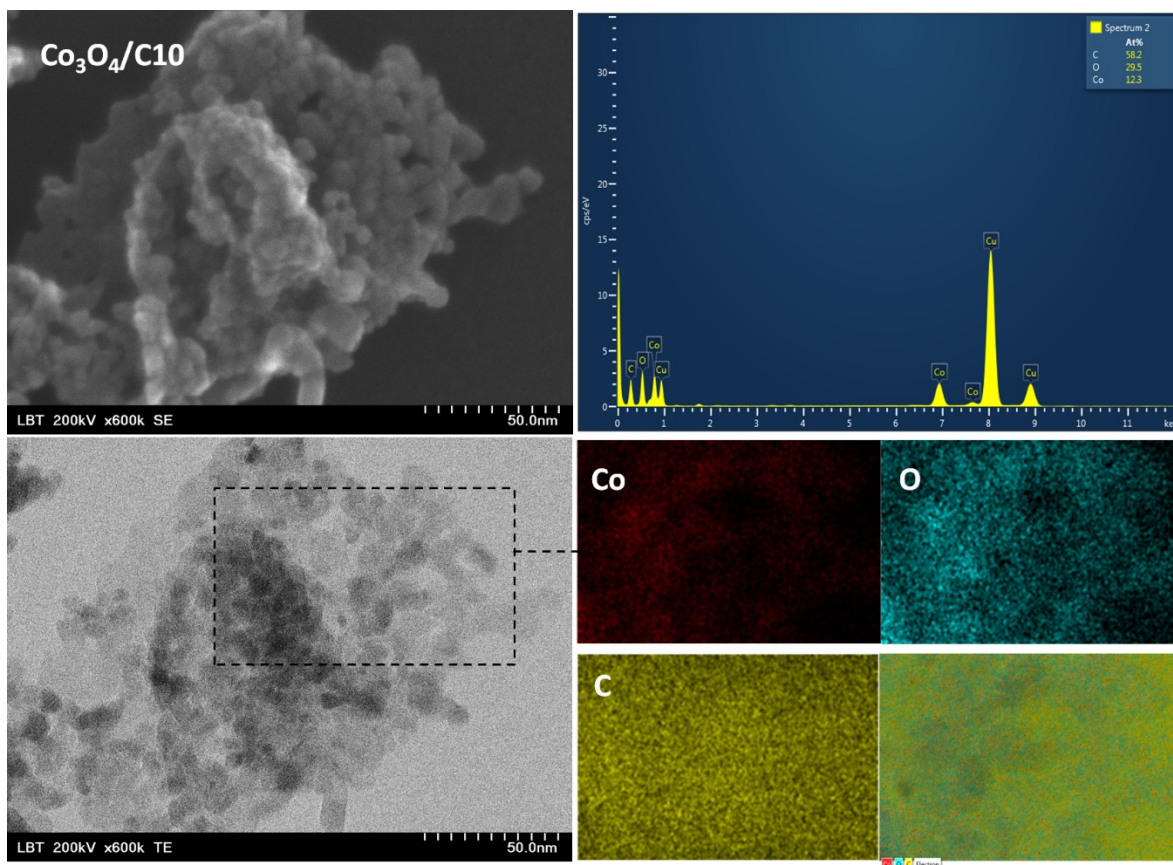
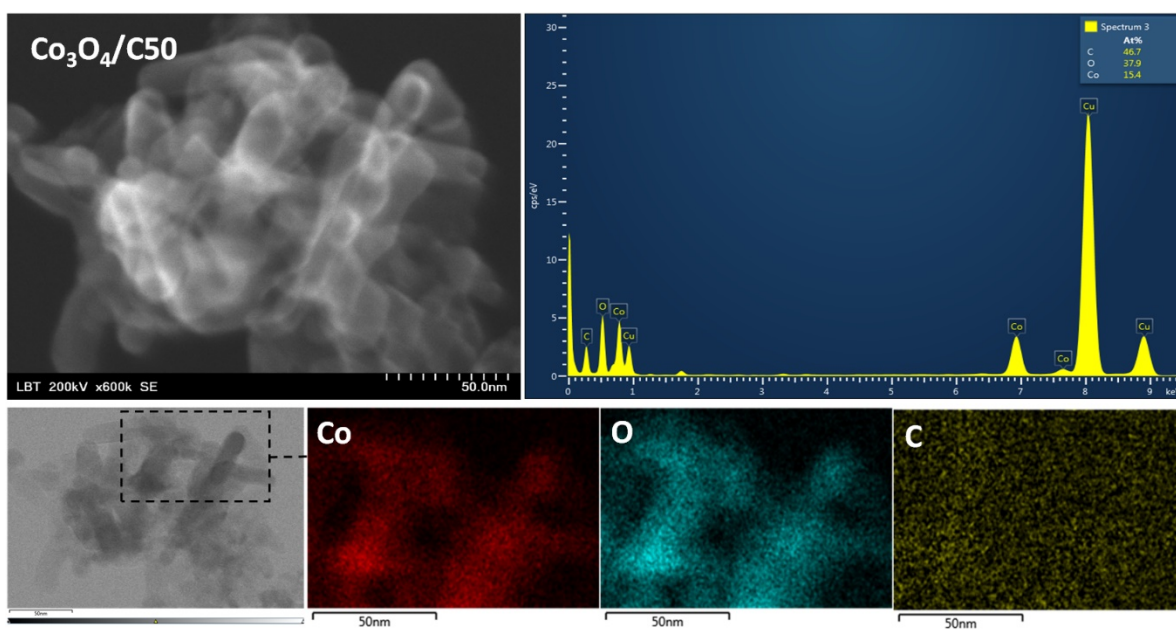


Figure S8: Particle size distribution for the  $\text{Co}_3\text{O}_4/\text{C10}$  nanocomposite, calculated from TEM image.





**Figure S9:** S-TEM images and elementary EDX mapping collected for  $\text{Co}_3\text{O}_4/\text{C10}$  nanocomposite.



**Figure S10:** S-TEM images and elementary EDX mapping collected for  $\text{Co}_3\text{O}_4/\text{C50}$  nanocomposite.



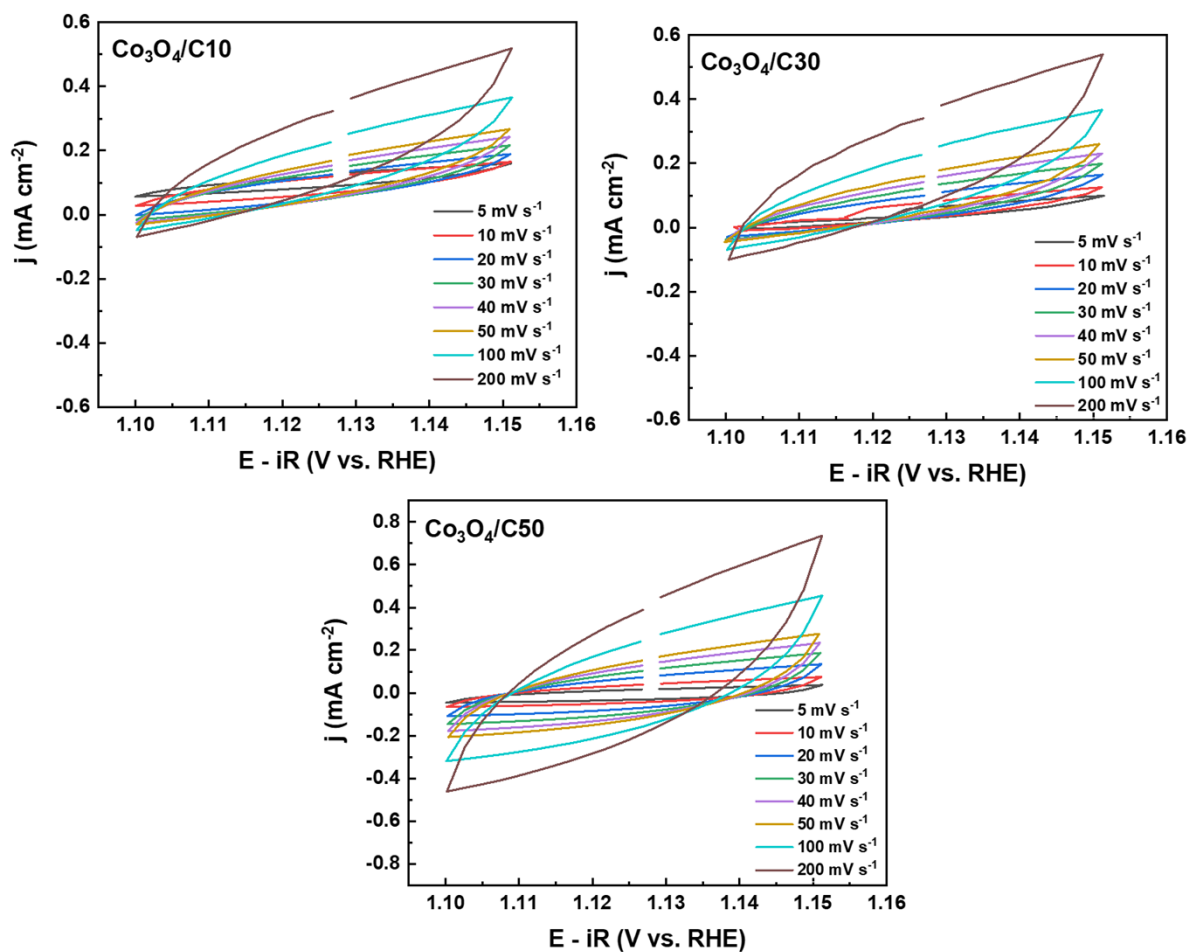


Figure S11: CV curves of  $\text{Co}_3\text{O}_4/\text{C}$  composites.

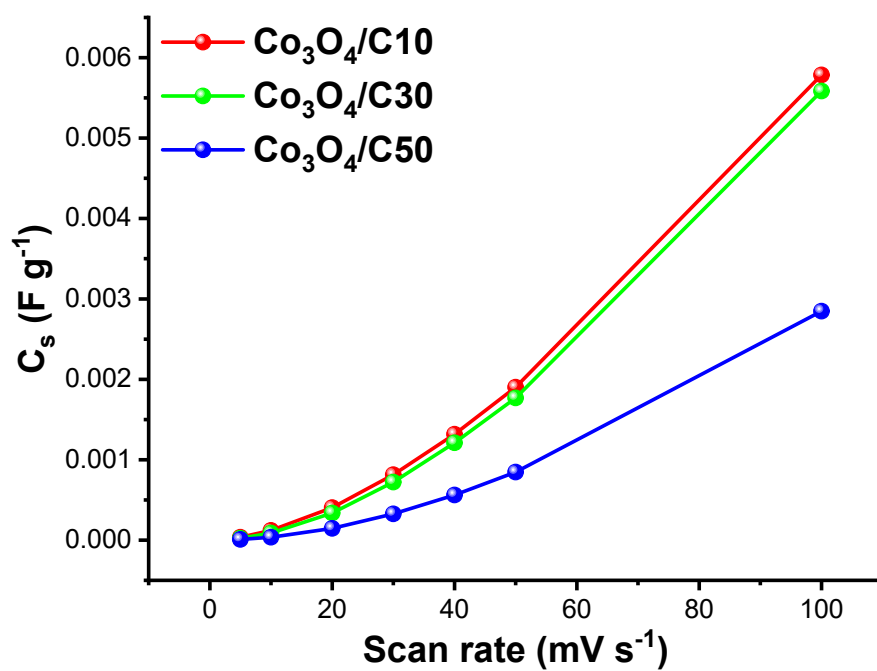


Figure S12: Specific capacitances from CV data.

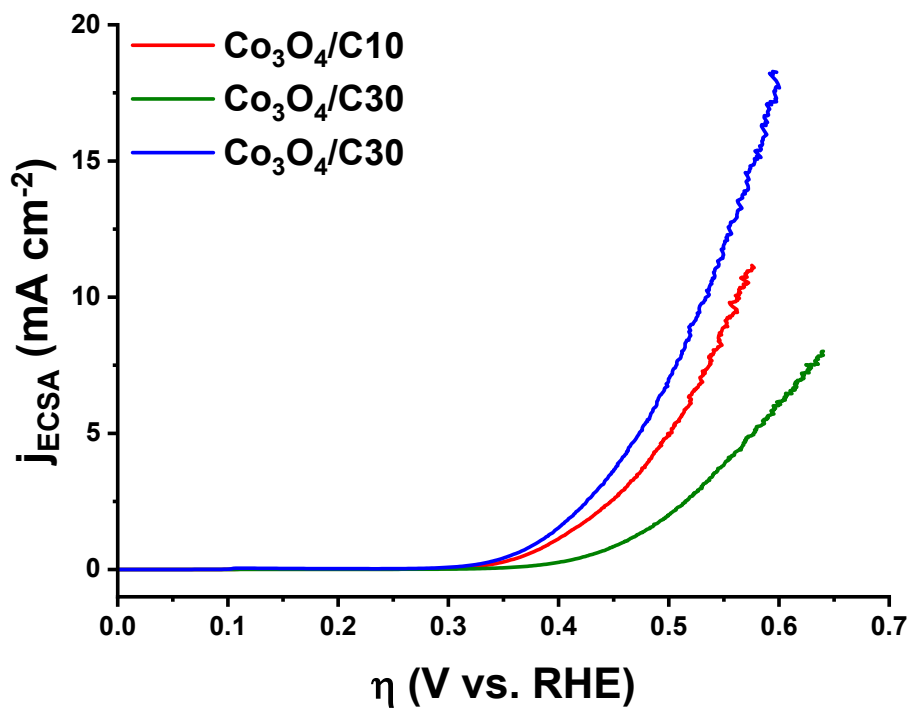


Figure S13: ECSA normalized LSV data.

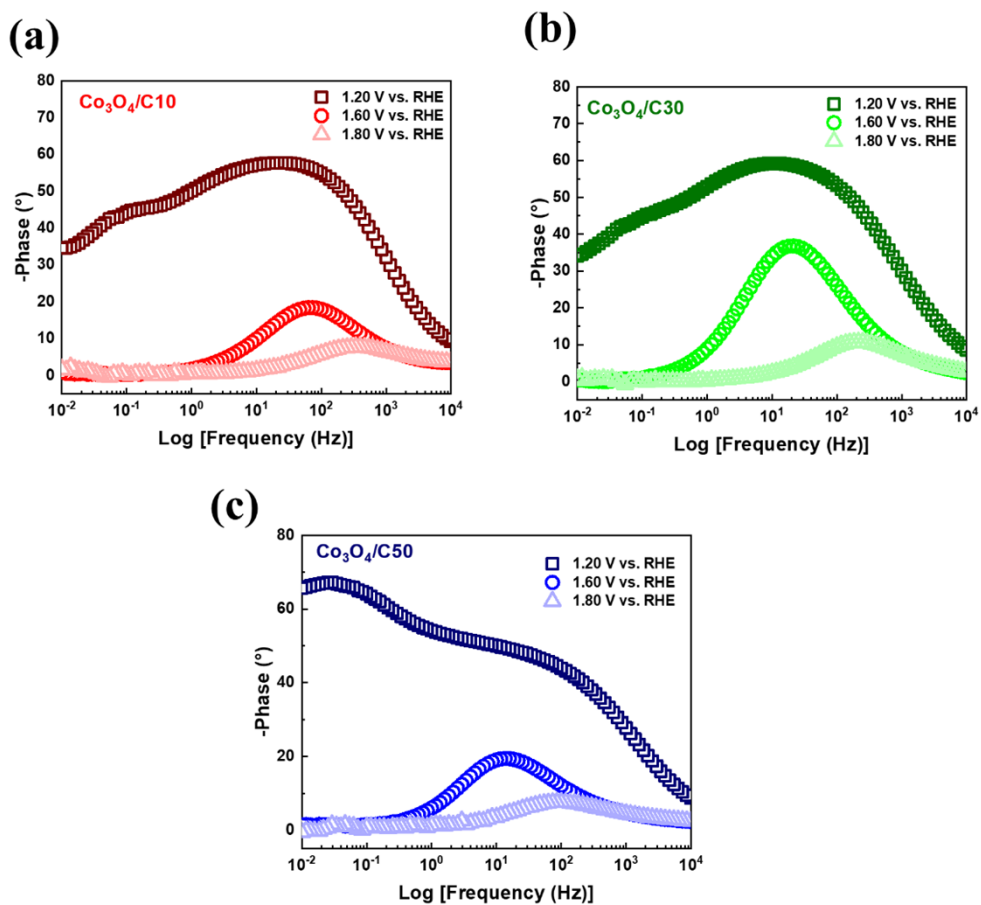


Figure S14: Bode plots obtained from EIS data for  $\text{Co}_3\text{O}_4/\text{C}$  composites.

**Table S3:** XPS deconvolution parameters for sample ZIF-67/C10.

Peak assignment	Position (eV)	FWHM	Area/(RSF x T x MFP) (eV s <sup>-1</sup> )
Co <sup>3+</sup> 2p <sub>3/2</sub>	780.48	4.46	255.702
Co <sup>3+</sup> 2p <sub>1/2</sub>	795.78	4.91	248.001
Co <sup>2+</sup> 2p <sub>3/2</sub>	778.28	1.75	127.757
Co <sup>2+</sup> 2p <sub>1/2</sub>	793.58	1.93	123.907
sat2	787.11	2.99	12.1062
sat4	804.1	4.5	23.4103
sat1	783.03	5.52	106.429
Co Auger	778.99	2.19	98.9171
sat 3	800.05	4.74	20.6222
Co Auger	776.22	1.5	10.2545

**Table S4:** XPS deconvolution parameters for sample Co<sub>3</sub>O<sub>4</sub>/C10.

Peak assignment	Position (eV)	FWHM	Area/(RSF x T x MFP) (eV s <sup>-1</sup> )
Co <sup>3+</sup> 2p <sub>3/2</sub>	780.25	3.8	919.04
Co <sup>3+</sup> 2p <sub>1/2</sub>	795.55	4.18	877.003
Co <sup>2+</sup> 2p <sub>3/2</sub>	778.44	2.51	460.109
Co <sup>2+</sup> 2p <sub>1/2</sub>	793.74	2.76	439.075
sat2	788.44	4.32	153.245
sat4	802	5.36	184.78
sat1	784.62	4.78	409.185
Co Auger	778.7	2.86	155.401
sat 3	800.97	2.93	26.2153
Co Auger	775.94	3.56	103.6

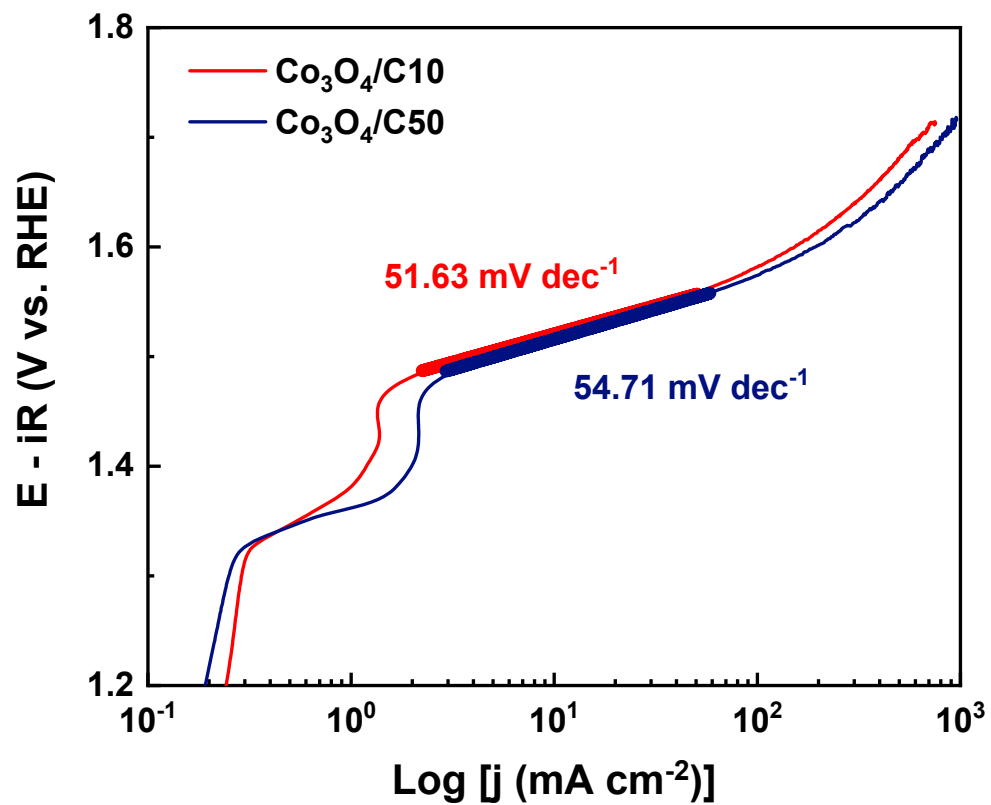


**Figure S15:** Tafel slopes for  $\text{Co}_3\text{O}_4/\text{C10}$  and  $\text{Co}_3\text{O}_4/\text{C50}$  samples after chronopotentiometry experiments.

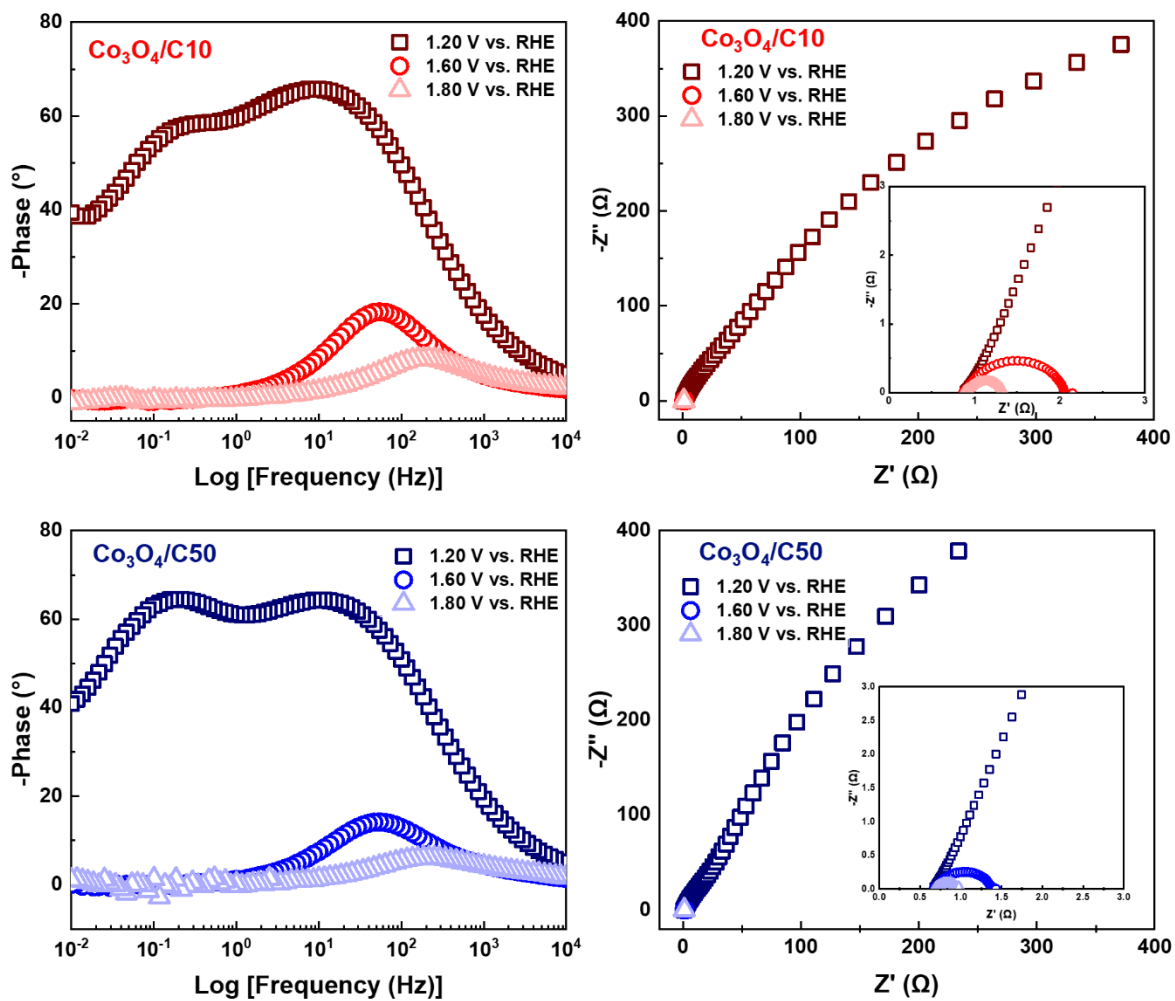


**Figure S16:** ESI data of the  $\text{Co}_3\text{O}_4/\text{C10}$  and  $\text{Co}_3\text{O}_4/\text{C50}$  samples after chronopotentiometry experiments.

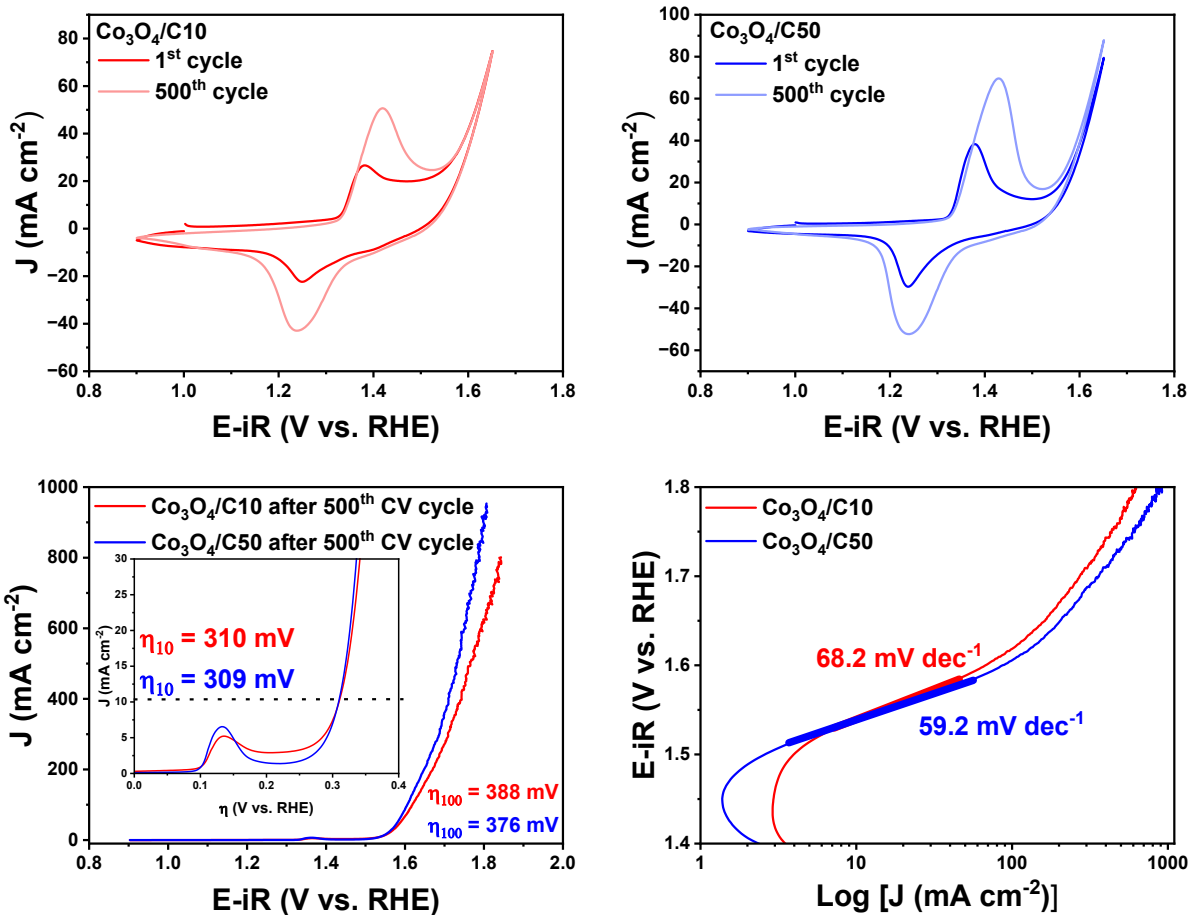


**Figure S17:** The first and 500<sup>th</sup> CV cycle, LSV and Tafel slope data after the 500<sup>th</sup> CV cycle.